

BUHEP-99-25
McGill-99/31
OITS-681
SHEP-99-16

On the QCD Ground State at High Density

Nick Evans¹, James Hormuzdiar², Stephen D.H. Hsu³, Myck Schwetz⁴

¹*Department of Physics, University of Southampton, Southampton, S017 1BJ, UK.*

²*Department of Physics, McGill University, 3600 University, Montreal, Quebec, H3A 2T8, USA.*

³*Department of Physics, University of Oregon, Eugene OR 97403, USA*

⁴*Department of Physics, Boston University, Boston, MA 02215, USA.*

October, 1999

Abstract

We investigate the possible ground states of QCD at asymptotic densities, where the theory is expected to exhibit color superconductivity. We characterize the color-flavor structure of possible diquark condensates, and find those that are energy extrema by solving the weak-coupling Dyson-Schwinger equations, including Landau damping and the Meissner effect. We show that, as previously anticipated, in the two flavor case the vacuum breaks $SU(3)$ color to $SU(2)$ and in the three flavor case the vacua with color-flavor locking (CFL) have the lowest energy. We identify a number of relatively flat directions in the potential along which the pattern of gauge symmetry breaking changes and parity is violated. We discuss possible phenomenological consequences of our results.

1 Introduction

QCD at high density and low temperature is a color superconductor [1]-[20] characterized by the formation of a diquark condensate in the attractive $\bar{3}$ color channel. The condensation is analogous to Cooper pairing in ordinary superfluids or superconductors, and occurs even via arbitrarily weak attractive interactions due to the presence of a Fermi surface [5, 6, 21]. Recently it was discovered [7, 8, 17, 18, 20] that long range magnetic fluctuations enhance the condensation, leading to a gap which behaves as

$$\Delta \sim \mu g^{-5} \exp\left(-\frac{3\pi^2}{\sqrt{2}g}\right) \quad (1)$$

in the weak coupling (small g , or large μ) limit. In this limit (1) is the gauge invariant, leading order result of a systematic expansion in powers of g . The properties of the condensate are easy to determine in the case of two quark flavors. Because the condensate occurs between pairs of either left (LL) or right (RR) handed quarks in the $J=L=S=0$ channel [20], and the $\bar{3}$ color channel is antisymmetric, the quarks must pair in the isospin singlet ($ud - du$) flavor channel. However, even in this case there is a subtlety, as the relative color orientations of the LL and RR condensates are not determined by the usual leading order analysis. A misalignment of these condensates violates parity, and further breaks the gauge group beyond $SU(3)_c \rightarrow SU(2)_c$. As we will discuss below, an analysis of the Meissner effect is necessary to determine the relative orientation. There are thus a number of unstable configurations of only slightly higher energy with different color-flavor orientations (and hence different symmetry breaking patterns), leading to the possibility of disorienting the diquark condensate. We include a discussion of possible phenomenological signals associated with these phenomena.

The generalization to three flavors is far from straightforward. Again, one can show that the condensate must occur in the $J=L=S=0$ and color $\bar{3}$ channel. The Pauli principle then requires that the flavor structure again be antisymmetric $\sim (q_i q_j - q_j q_i)$, for quarks of flavor i, j . Thus, one can have combinations of condensates which are in the $\bar{3}$ of both color and flavor $SU(3)_L$ or $SU(3)_R$. Due to the chirality preserving nature of perturbative gluon exchange, there is no mixing of LL and RR condensates, which form independently. One can immediately see that there are a number of possibilities. For example, the condensates for the three flavors and both chiralities might all align in color space, leading to an $SU(3)_c \rightarrow SU(2)_c$ breaking pattern. A more complicated condensate has been proposed [13, 16] called Color Flavor Locking (CFL), in which the $\bar{3}$ color orientations are “locked” to the $\bar{3}$ flavor orientation.

In this paper we determine the nature of the energy surface governing the various color-flavor orientations of the condensate. Let us begin by characterizing the color-flavor config-

uration space of condensates. We consider the ansatz

$$\Delta_{ij}^{ab\ L,R} = A_k^c\ ^{L,R} \epsilon^{abc} \epsilon_{ijk} \quad , \quad (2)$$

where a,b are color and i,j flavor indices. L and R denote pairing between pairs of left and right handed quarks, respectively. Under color and flavor A transforms as

$$A^L \rightarrow U_c A^L V^L \quad , \quad (3)$$

where U_c is an element of $SU(3)_c$ and V^L of $SU(3)_L$. A similar equation holds for A^R . It is always possible to diagonalize A^L by appropriate choice of U_c and V^L :

$$A^L = \begin{pmatrix} a & 0 & 0 \\ 0 & b & 0 \\ 0 & 0 & c \end{pmatrix} \quad . \quad (4)$$

Generically, there does not exist a V^R which diagonalizes A^R in this basis. In the CFL case, where the diagonalized A^L is proportional to the identity, $a = b = c$, it is easy to show that one can choose V^R such that $A^R = \pm A^L$. These two configurations are related by a $U(1)_A$ rotation (see section 3). Hence, they are degenerate in the high density limit where gluon exchange dominates. Instanton effects, important at intermediate density, favor $A^R = A^L$. Note that parity, if unbroken, requires $A^L = A^R$, and hence implies simultaneous diagonalizability.

In what follows we consider the potential vacua parametrized by a,b,c. First, we use the Dyson-Schwinger (gap) equation to determine which of these configurations are energy extrema. Next, we compute the energies of the extrema to determine the true groundstate. A similar analysis has been carried out by Schäfer and Wilczek [16] in the approximation where gluon interactions are replaced by local four fermion interactions. They concluded that the CFL vacuum had the lowest energy. Here, we include the gluons in the analysis, introducing long range color-magnetic fluctuations (controlled by Landau damping) and Meissner screening into the gap equation and vacuum energy calculations.

We find that the CFL vacua remains the lowest energy state, at least at asymptotically high densities where the calculation is reliable. The Meissner effect is a small correction to the vacuum energy at asymptotic densities. At lower densities where the gauge coupling is large the Meissner terms become more important and tend to disfavor CFL relative to the absence of a condensate. We do not know whether they are ever sufficient to remove the superconducting phase but they will lower the energy difference between the vacuum and unstable condensates with different color and flavor breaking patterns. Configurations which satisfy the gap equations but are not the global minimum of energy are presumably saddlepoints, since they are continuously connected to the CFL vacuum via color and flavor rotations.

2 Gap Equation

In this section we determine the subset of parameter space for which our ansatz (4) satisfies the gap equation. Because the gap equation results from the extremization of the effective action, its solutions are energy extrema. At asymptotically high densities (weak coupling) the diagrams (a)-(c) in figure 1 give the leading approximation to the effective action. Note that in these diagrams the quark propagators include the diquark condensate (see (10) below), and the gluon propagators include Landau damping, but *not* the Meissner effect. The latter arises from the condensate-dependence of quark loops in diagrams (c) and (d). The resulting gap equation (figure 2, with condensate shown explicitly at lowest order in Δ) is given by

$$S^{-1}(q) - S_0^{-1}(q) = ig^2 \int \frac{d^4k}{(2\pi)^4} \Gamma_\mu^A S(k) \Gamma_\nu^B D_{AB}^{\mu\nu}(k-q), \quad (5)$$

where

$$\Gamma_\mu^A = \begin{pmatrix} \gamma_\mu T^A & 0 \\ 0 & C(\gamma_\mu T^A)^T C^{-1} \end{pmatrix}. \quad (6)$$

$D_{AB}^{\mu\nu}$ is the gluon propagator, include the effects of Landau damping and Debye screening (we assume Feynman gauge throughout):

$$D^{\mu\nu} = \frac{1}{q^2 + G} P_T^{\mu\nu} + \frac{1}{q^2 + F} P_L^{\mu\nu}, \quad (7)$$

where $P_{T,L}$ are transverse and longitudinal projectors. The analytic forms of F and G are given below in (15). The small $\frac{q_0}{q}$ expansion of G leads to the Landau damped magnetic gluon propagator

$$D_T^{\mu\nu}(q_0, q) = \frac{P_T^{\mu\nu}}{q^2 + i\frac{\pi}{2}m_D^2 \frac{|q_0|}{q}}, \quad (8)$$

while the expansion of F leads to the usual longitudinal propagator, with Debye screening: $m_D^2 = N_f \frac{q^2 \mu^2}{2\pi^2}$.

We will restrict the color group structure in the gap equation to the attractive anti-symmetric $\bar{3}$ channel:

$$T_{ab}^A T_{cd}^A \rightarrow \frac{1}{3} (\delta_{ac}\delta_{bd} - \delta_{ab}\delta_{cd}), \quad (9)$$

which projects out the anti-symmetric part of $S(k)$ in color space in the gap equation. Here S is the fermion propagator for the spinor (ψ_a^i, ψ_a^{iC}) with i a flavor index and a a color index.

For the three flavor case S can be written explicitly as an 18×18 matrix in color flavor space. The inverse propagator may be written

$$S^{-1}(q) = \begin{pmatrix} \not{q} + \not{k} & \gamma_0 \Delta^\dagger \gamma_0 \\ \Delta & \not{q} - \not{k} \end{pmatrix} \quad (10)$$

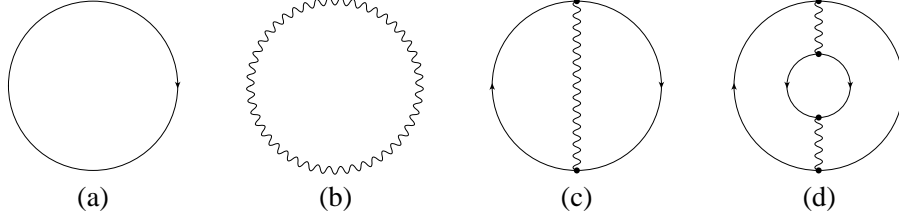


Figure 1: Vacuum energy diagrams

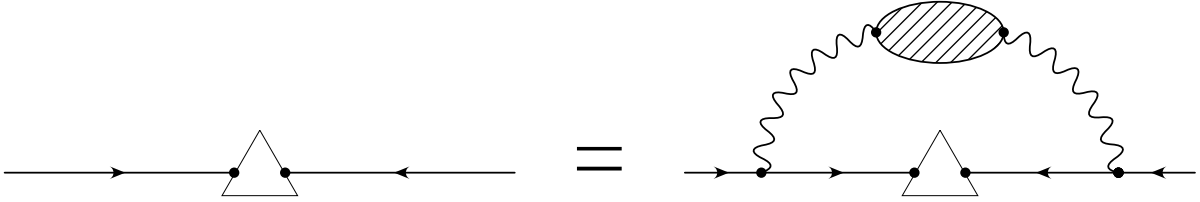


Figure 2: Dyson-Schwinger equation

where $\not{k} = \mu\gamma_0$. Δ is a 9×9 matrix which for the ansatz (4) takes the form

$$\Delta = \begin{pmatrix} 0 & 0 & 0 & 0 & c & 0 & 0 & 0 & b \\ 0 & 0 & 0 & -c & 0 & 0 & 0 & 0 & 0 \\ 0 & 0 & 0 & 0 & 0 & 0 & -b & 0 & 0 \\ 0 & -c & 0 & 0 & 0 & 0 & 0 & 0 & 0 \\ c & 0 & 0 & 0 & 0 & 0 & 0 & 0 & a \\ 0 & 0 & 0 & 0 & 0 & 0 & 0 & -a & 0 \\ 0 & 0 & -b & 0 & 0 & 0 & 0 & 0 & 0 \\ 0 & 0 & 0 & 0 & 0 & -a & 0 & 0 & 0 \\ b & 0 & 0 & 0 & a & 0 & 0 & 0 & 0 \end{pmatrix} \quad (11)$$

Because we are dealing with a diquark condensate the non-trivial part of the gap equation involves the lower left 9×9 block. We will refer to this sub-block of the propagator S as S_{21} .

For a particular ansatz Δ to be a solution to the gap equation we require that the color antisymmetric part of $T^A S_{21}(k) T^A$ (corresponding to the $\bar{3}$ channel) be proportional in color-flavor space to $S^{-1}(q) - S_0^{-1}(q) = \Delta(q)$, which appears on the LHS of the gap equation. This requires some justification, as the matrices that appear on the RHS of the gap equation appear inside the integral. If, for simplicity, we restrict ourselves to ansätze which correspond to constant color-flavor matrices times a function of momenta, then this condition is implied. In principle, there can be more exotic solutions in which color and flavor orientations rotate in momentum space, however it seems unlikely that such solutions exist. We note that the equality must hold for all values of the external momentum q , and that the set of functions $D(k - q)$ are likely to form a complete basis for functions of k , since

they are essentially smeared delta functions of $(\mathbf{k}-\mathbf{q})$. Thus by taking appropriate linear combinations of the gap equation we can see that $T^A S_{21}(k) T^A$ must be proportional to Δ when integrated against any arbitrary function of \mathbf{k} . Hence the proportionality must hold without the integral.

The propagator may be found by inverting the sparse matrix in (10) using Mathematica. Only three ansätze satisfy our condition: $a = b = c$; $a = b, c = 0$; $b = c = 0$. We refer to these solutions as (111) (color-flavor locking), (110) ($3 \rightarrow 0$ breaking) and (100) ($3 \rightarrow 2$ breaking) respectively.

For these ansätze the color antisymmetric part of $T^A S_{21}(k) T^A$ has the form of a constant multiplying the matrix form (11) with a, b, c set to 0 or 1 as is appropriate for the ansatz. The constants are (here $l^2 = (|\vec{k}| - \mu)^2$):

$$\begin{aligned}
(111) & : \frac{2\Delta}{(k_0^2 - l^2 + \Delta^2)} \frac{(k_0^2 - l^2 + 3\Delta^2)}{(k_0^2 - l^2 + 4\Delta^2)} \\
(110) & : \frac{\Delta}{(k_0^2 - l^2 + \Delta^2)} + \frac{\Delta}{(k_0^2 - l^2 + 2\Delta^2)} \\
(100) & : \frac{2\Delta}{(k_0^2 - l^2 + \Delta^2)} \tag{12}
\end{aligned}$$

The integral over l can be performed by contour integration, yielding the following gap kernels

$$\begin{aligned}
(111) & : \frac{2}{3} \frac{\Delta}{\sqrt{k_0^2 + \Delta^2}} + \frac{1}{3} \frac{\Delta}{\sqrt{k_0^2 + 4\Delta^2}} \\
(110) & : \frac{\Delta}{2\sqrt{k_0^2 + \Delta^2}} + \frac{\Delta}{2\sqrt{k_0^2 + 2\Delta^2}} \\
(100) & : \frac{\Delta}{\sqrt{k_0^2 + \Delta^2}} \tag{13}
\end{aligned}$$

Let us now simplify the gap equations. We neglect q_0 , as compared to $|\vec{q}|$, as well as anti-particle contributions (see, e.g., [18], for details). We obtain

$$\begin{aligned}
\Delta(p_0) = \frac{g^2}{12\pi^2} \int dq_0 \int d\cos\theta & \left(\frac{\frac{3}{2} - \frac{1}{2}\cos\theta}{1 - \cos\theta + (G + (p_0 - q_0)^2)/(2\mu^2)} \right. \\
& \left. + \frac{\frac{1}{2} + \frac{1}{2}\cos\theta}{1 - \cos\theta + (F + (p_0 - q_0)^2)/(2\mu^2)} \right) K(q_0), \tag{14}
\end{aligned}$$

where

$$F = 2m^2 \frac{q^2}{\vec{q}^2} \left(1 - \frac{iq_0}{|\vec{q}|} Q_0 \left(\frac{iq_0}{|\vec{q}|} \right) \right), \quad Q_0(x) = \frac{1}{2} \log \left(\frac{x+1}{x-1} \right),$$

$$G = m^2 \frac{iq_0}{|\vec{q}|} \left[\left(1 - \left(\frac{iq_0}{|\vec{q}|} \right)^2 \right) Q_0 \left(\frac{iq_0}{|\vec{q}|} \right) + \frac{iq_0}{|\vec{q}|} \right], \quad (15)$$

and $K(q_0)$ is one of the gap kernels from (13).

These gap equations can be solved numerically. We first present solutions neglecting the Meissner effect. The results for Δ vs p_0 are displayed in figures 3 and 4 for the three ansätze¹. (The spatial momentum \vec{p} is taken to lie on the Fermi surface.) The curves lie very close to each other but as we will see below give quite different contributions to the vacuum energy. Note that the gap solutions we obtain have broad support, from the Fermi surface to $l, k_0 \sim \mu$. However, this is likely a consequence of the approximations used in (14), in which all momenta are assumed to lie close to the Fermi surface.

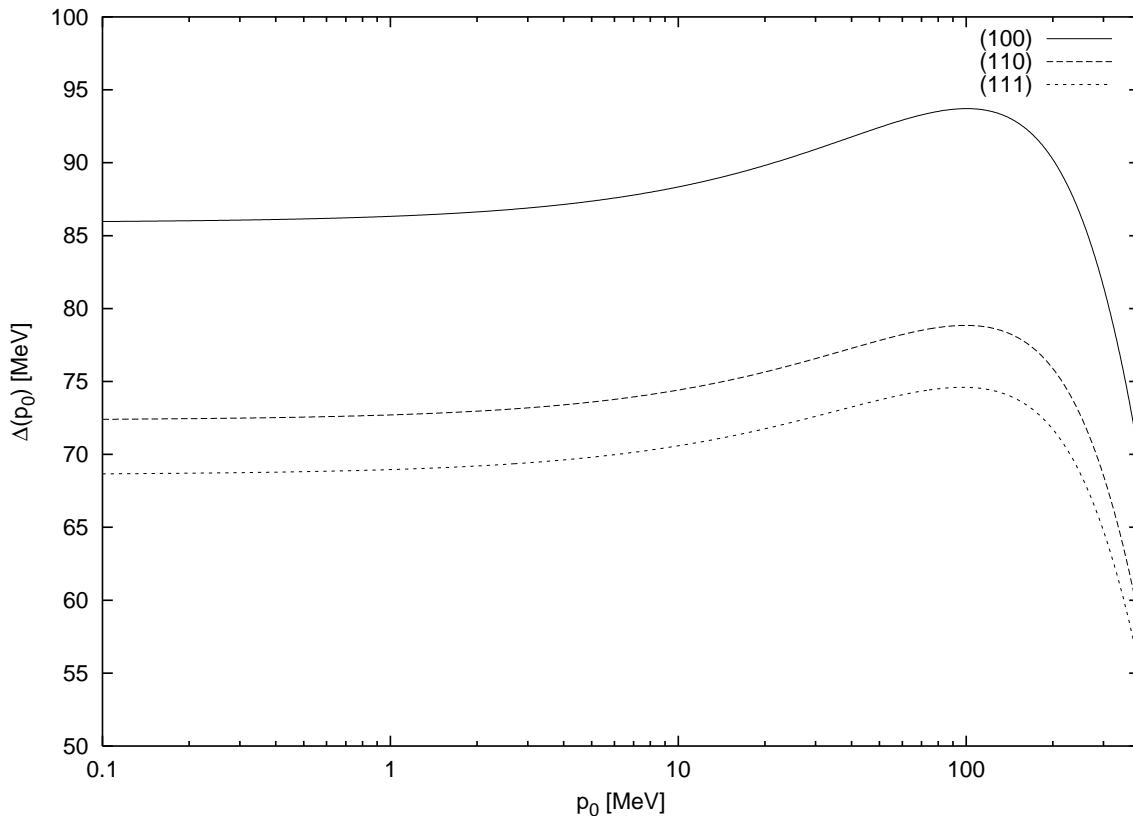


Figure 3: Gap Solutions for $\mu = 400$ MeV

A complete analysis must also include the Meissner effect, that is the screening of the gluons induced by the formation of the gap. The leading order contribution to the gluon

¹Our results differ somewhat in normalization from those of [18], although the shapes of the curves are in agreement.

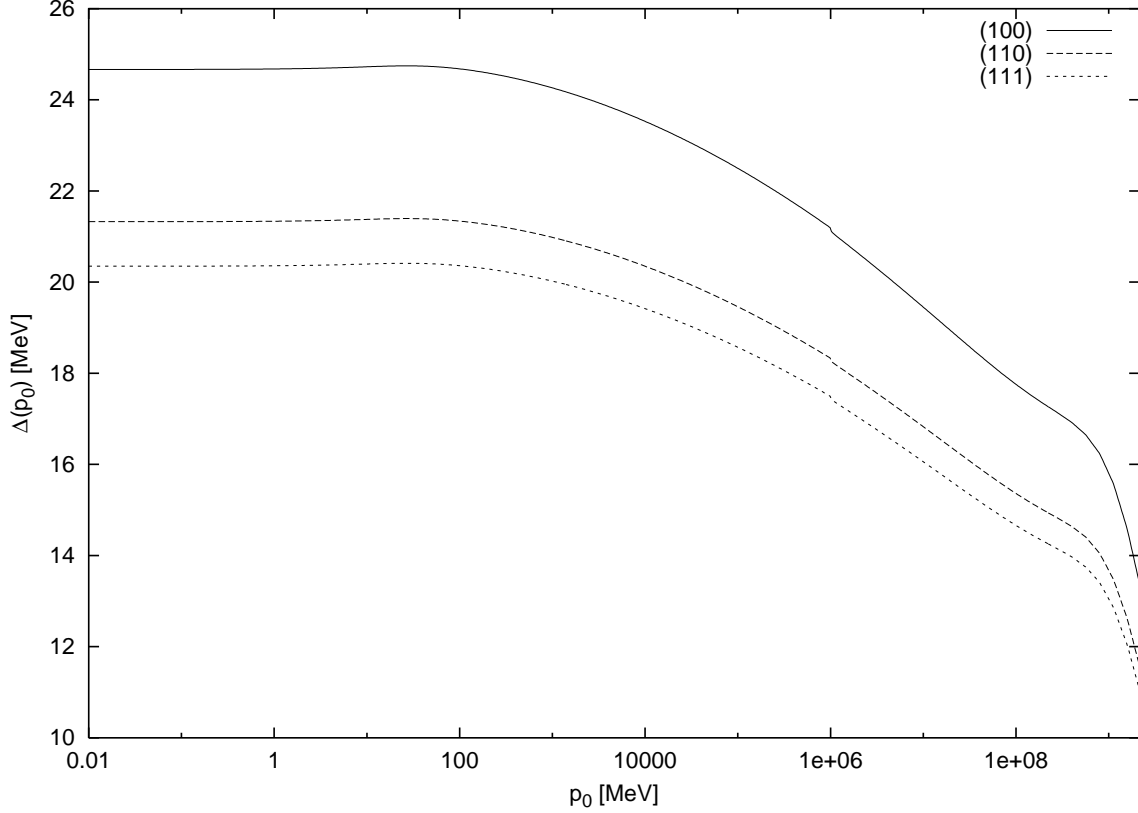


Figure 4: Gap Solutions for $\mu = 10^{10}$ MeV

vacuum polarization $P(k_0, k)$ comes from the off-diagonal terms in the fermion propagator-matrix

$$\delta P_{\mu\nu}(q_0, q) = g^2 \int \frac{d^4 k}{(2\pi)^4} \text{Tr} \left[\gamma_\mu S_{12}(k) C \gamma_\nu^T C^{-1} S_{21}(k - q) \right]. \quad (16)$$

where we have dropped the group theory factors. It is convenient to use the formalism of [9] which exploits simplifications due to decomposition of the fermion propagator into a sum of projections onto different chirality and helicity channels. After some tedious algebra one gets for (16)

$$\delta P_{ij}(q_0, q) = 2g^2 \int \frac{d^4 k}{(2\pi)^4} \frac{|\Delta|^2}{k_0^2 + \epsilon(k)^2} \frac{g_{ij} + \frac{1}{2}(\hat{k}_i \widehat{k} - q_j + \hat{k}_j \widehat{k} - q_i)}{(k_0 - q_0)^2 + \epsilon(k - q)^2}, \quad (17)$$

where $\hat{k} = \vec{k}/|\vec{k}|$ and $\epsilon(k)^2 = (|\vec{k}| - \mu)^2 + |\Delta|^2$. It is easier to compute the contribution to the magnetic gluon mass G directly applying the transverse projector $P_{ij}^T = (\delta_{ij} - \hat{q}_i \hat{q}_j)$ to the gluon vacuum polarization while using the HDL approximation (the momentum in the

loop $k \sim \mu$ and is much bigger than the momentum transfer q) [22]:

$$\delta G(q_0, q) = \frac{1}{2} P_{ij}^T \delta P_{ij}(q_0, q) = g^2 \int \frac{d^4 k}{(2\pi)^4} \frac{|\Delta|^2}{k_0^2 + \epsilon(k)^2} \frac{1 + \hat{k} \cdot \hat{q}}{(k_0 - q_0)^2 + \epsilon(k - q)^2} \quad . \quad (18)$$

Further simplification comes after switching on a small temperature and performing a summation over frequencies [22]. Note that, because the system is already decomposed into particles and anti-particles about the Fermi surface, one should apply the summation formulae as if $\mu = 0$. Finally, one finds

$$\delta G(q_0, q) = 2 \frac{g^2 |\Delta|^2}{(2\pi)^3} \int \frac{d^3 k}{\epsilon(k) \epsilon(k - q)} \frac{\epsilon(k) + \epsilon(k - q)}{q_0^2 + (\epsilon(k) + \epsilon(k - q))^2} \quad . \quad (19)$$

One can see, either by analytical approximation or numerical evaluation, that $\delta G(q_0, q)$ is of order m_D^2 for $q_0 \sim q \sim \Delta$, and falls off like $1/q_0$ or $1/q$ as either become large [17]. While this is of the same order as Landau damping, numerical evaluation shows that the Meissner contribution is somewhat smaller.

As we are only interested in the size of the contribution of the Meissner effect, we use the following approximation, which is an overestimate of the effect:

$$\delta G(q_0, q) \simeq m_D^2 \frac{\Delta_0}{\sqrt{q^2 + q_0^2 + \Delta_0^2}} \quad , \quad (20)$$

where Δ_0 is the maximum value of the function $\Delta(k_0, k)$. The gap equations were numerically solved for all three gap kernels, and the results are shown in figures 5 and 6. The effect is to decrease the size of the condensate but it is a small perturbation on the solutions obtained previously.

3 Vacuum Energies

To determine which of the above gaps is the true minimum energy state we must calculate the vacuum energy, which receives contributions from vacuum to vacuum loops of both quarks and gluons (figure 1). We use the CJT effective potential, which is a function of condensates [23]:

$$\begin{aligned} V(S, D) &= -i \int \frac{d^4 p}{(2\pi)^4} \left[\text{tr} \ln S(p)/S_0(p) + \text{tr}(1 - S(p)/S_0(p)) - \frac{i}{2} \text{tr} \ln D(p)/D_0(p) \right. \\ &\quad \left. - \frac{i}{2} \text{tr}(1 - D(p)/D_0(p)) \right] + \frac{i}{2} \int \int \frac{d^4 p}{(2\pi)^4} \frac{d^4 k}{(2\pi)^4} \left[\text{tr} \Gamma S(p) \Gamma S(p + k) D(k) \right] \\ &\quad + \dots \end{aligned} \quad (21)$$

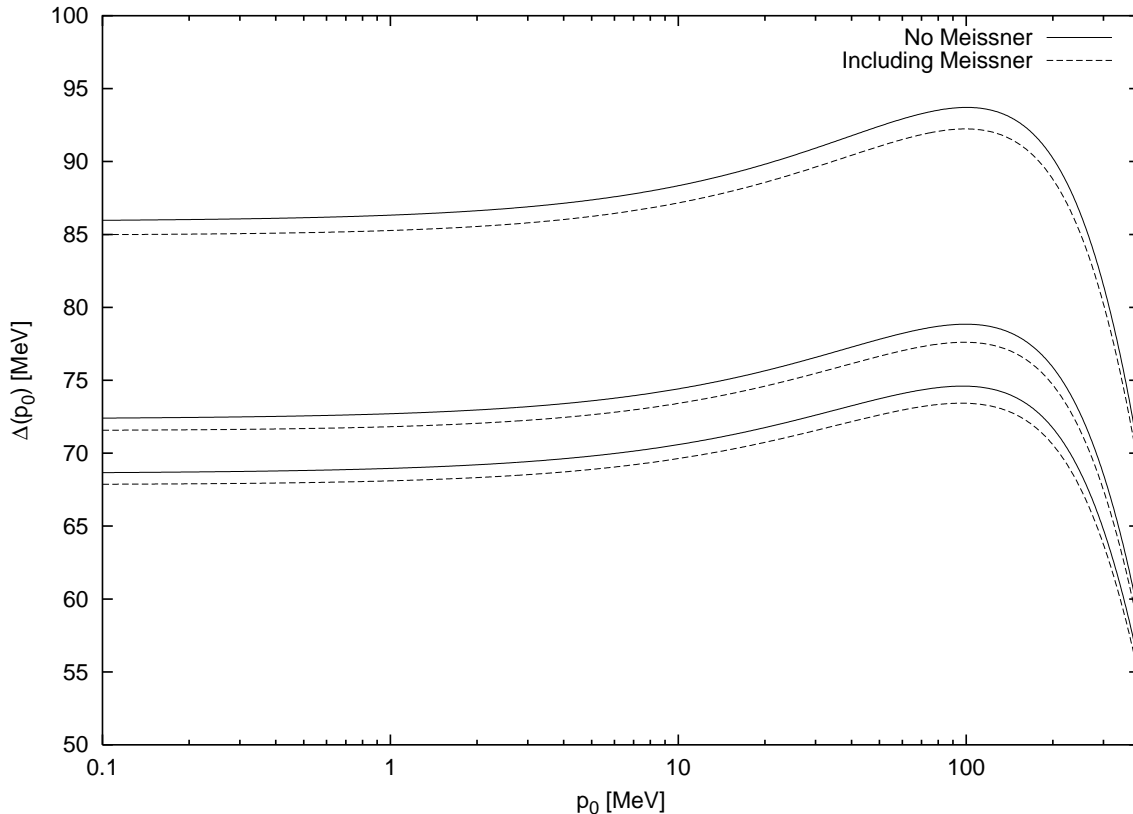


Figure 5: Gap Solutions for $\mu = 400$ MeV

where for convenience we suppress appropriate color, flavor and Dirac indices. S_0 and S correspond to bare and full fermion propagators, D_0 and D to bare and full gluon propagators and Γ to full vertices. The ellipsis denote gluon self-interaction loops and terms which are higher order in g . In our approximation, which is essentially Hartree-Fock (lowest order in coupling), the Γ 's become bare vertices.

Extremizing with respect to appropriate propagators and vertices one obtains a set of gap equations. The fermion gap equation is the one we studied in the previous section, while the gluon gap equation produces Landau damping. We wish to compare values of $V(S, D)$ corresponding to our three solutions to determine which one is the true vacuum². It is easy to show that the value of the effective potential evaluated on the gap solution (S^*, D^*) in the Hartree-Fock approximation is given by:

$$V(S^*, D^*) = -i \int \frac{d^4 p}{(2\pi)^4} \text{tr} \ln S(p) / S_0(p) . \quad (22)$$

²The difference in energies V will be gauge invariant, whereas actual values are not.

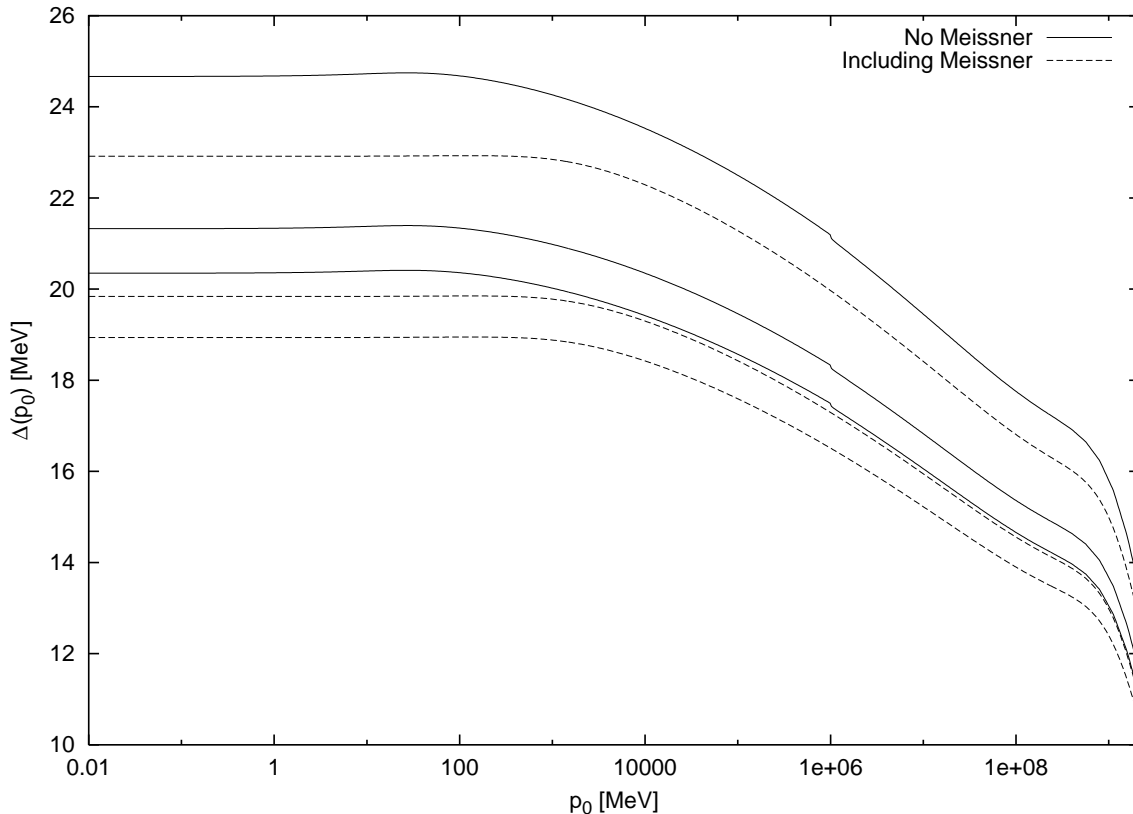


Figure 6: Gap Solutions for $\mu = 10^{10}$ MeV

Diagrammatically, this is equivalent to the graph of figure 1(a) when evaluated on the gap solution.

The fermion loops are most easily calculated by going to a basis where $S_0 S^{-1}$ is diagonal in color-flavor space. Note that the gap matrix Δ has non-trivial Dirac structure that must be accounted for [9]:

$$\Delta = \Delta_1 \gamma_5 P_+ + \Delta_2 \gamma_5 P_- \quad , \quad (23)$$

where P_{\pm} are particle and anti-particle projectors. Our analysis has been restricted to the particle gap function Δ_1 . The anti-particle gap function Δ_2 has its support near $k_0 \sim 2\mu$, and its contribution to the vacuum energy is suppressed. There are 18 eigenvalues, which occur in 9 pairs. The product of each pair is of the form

$$- \left(1 + a \frac{\Delta^2(k_o, k)}{k_0^2 + (|\vec{k}| - \mu)^2} \right) \quad , \quad (24)$$

where a is an integer. For our three cases we obtain the following sets of eigenvalues:

$$(111) \quad \rightarrow \quad 8 \times \{a = 1\} \quad , \quad 1 \times \{a = 4\}$$

$$\begin{aligned}
(110) &\rightarrow 4 \times \{a = 1\} , 2 \times \{a = 2\} \\
(100) &\rightarrow 4 \times \{a = 1\}
\end{aligned}
\tag{25}$$

The binding energy is of order

$$E_q \sim - \int d^3k dk_0 \ln \left[1 + a \frac{\Delta^2(k_0, k)}{k_0^2 + (k - \mu)^2} \right] \tag{26}$$

$$\sim -a \mu^2 \Delta_0^2 , \tag{27}$$

where Δ_0 is the maximum value of the gap function $\Delta(k_0, k)$, which has rather broad support in both energy and momentum space away from the Fermi surface, extending to $k_0, k \sim \mu$. A more precise answer than (26) requires numerical evaluation, but it is clear that the result scales with a and has only a weak (logarithmic) dependence on the variations in the shape of $\Delta(k_0, k)$. Substituting our numerical results for the gaps in the three cases, it is easy to establish that

$$E(111) < E(110) < E(100) . \tag{28}$$

Gluon loops corresponding to figure 1(b) yield a smaller contribution to the vacuum energy. To compute this energy we must use the gluon propagator suitably modified by the Meissner effect, which as we described above leads to the vacuum polarization $P(k_0, k)$. We obtain

$$E_g = \frac{3}{64\pi^3} \int dk_0 dk k^2 \ln \left[1 + \frac{P(k_0, k)}{k_0^2 + k^2} \right] . \tag{29}$$

To estimate the result of this integral it is necessary to use the properties of $P(k_0, k)$. Recall that $P(k_0, k)$ falls off like $m_D^2 \Delta_0 / k$ at $k \gg \Delta_0$, and similarly at large k_0 [17]. The dominant region of integration is therefore $k_0 \sim \Delta_0$ and $k_* \ll k \ll \mu$, where $k_* = m_D^{2/3} \Delta_0^{1/3}$ is the momentum scale familiar from Landau damping. From this region of integration we obtain

$$E_g \sim m_D^2 \Delta_0^2 \ln(\mu/k_*) \sim g\mu^2 \Delta_0^2 , \tag{30}$$

since $\ln k_* \sim 1/g$. The result is parametrically smaller than the quark contribution. Note that this contribution to the energy is positive and hence prefers the least possible breaking of the color gauge symmetry. If this term were the dominant one then it would disfavor the formation of a condensate and the CFL vacuum would be the highest energy state! At asymptotic densities it is not the dominant term and the analysis from the quark loops stands. At lower densities, where the coupling is large, these contributions to the energy become more important but we lose control of the calculation. Their effect is to lower the energy gap between the CFL vacuum and disoriented states with different color and flavor symmetry breaking patterns.

The contribution we just computed to E_g still cannot differentiate between relative color rotations between the LL and RR diquark condensates. This is because the energy E_g depends on the sums of the squares of the gauge boson masses induced. In order to be sensitive to LR coupling effects, it is necessary that both LL and RR contributions to $P(k_0, k)$ appear simultaneously in the vacuum energy contribution. The first such graph is that of figure 1(d), and it is of the form

$$E_g^{LR} \sim \int dk_0 dk k^2 \ln \left[1 + \left(\frac{P(k_0, k)}{k_0^2 + k^2} \right)^2 \right] . \quad (31)$$

This integral is dominated by the region $k_0 \sim \Delta_0, k \sim k_*$, leading to the result

$$E_g^{LR} \sim m_D^2 \Delta_0^2 \sim g^2 \mu^2 \Delta_0^2 . \quad (32)$$

This effect is further suppressed by a power of the coupling constant. We see that in the weak coupling limit the vacuum energy required to disorient the LL and RR condensates in color space is rather small. This suggests that even at asymptotic densities in the two flavor case it might be possible to disorient the diquark condensates from their lowest energy configuration. We have yet to determine what this lowest energy configuration is, and hence whether parity is violated in the two flavor case. In principle, one should minimize E_g^{LR} as a function of the relative LL and RR color orientation. Instead, we will give a simple argument that the condensates prefer to align. We noted in the last section that including the Meissner screening in the gluon propagator leads to a decrease in the gap size. This is a small effect at weak coupling, and was negligible compared to the color-flavor structure of the quark propagator. However, in determining LL-RR alignment it is the main effect. In the two flavor case none of the gluons responsible for the attractive interaction are Meissner screened, as long as the LL and RR condensates align. That is the quarks which condense are those that transform under the unbroken $SU(2)$ subgroup of $SU(3)_c$. However, any misalignment leads to the LL condensate screening the RR channel and vice versa, decreasing the condensates and thereby increasing the energy. Hence in the two flavor case the condensates prefer to align and parity is preserved. In the three flavor case CFL gives all of the gauge bosons a mass and this effect is absent.

In both the two and three flavor cases there remains the possibility of parity violation through a phase associated with the $U(1)_A$ symmetry [2, 5, 8]. Only instanton effects (highly suppressed at asymptotic densities) can distinguish these vacua. At lower densities instanton effects are expected to strongly break the $U(1)_A$ symmetry, since the η' mass is dominated by these effects at zero density.

4 Conclusions and Phenomenology

In this paper we analyzed the possible ground states of QCD at asymptotic densities. We verified that in the two flavor case, the symmetry breaking pattern is $SU(3)_c \rightarrow SU(2)_c$, while in the three flavor case, color flavor locking has the lowest vacuum energy. In neither case is parity spontaneously violated until the density is strictly infinite [5, 8].

Our analysis of the energy surface governing color superconductivity suggests possible experimental signatures in heavy ion collisions. In particular the existence of relatively flat directions along which color and flavor symmetry breaking patterns change raises the possibility of domains of disoriented condensates, each with distinct hadronization properties. In the two flavor case the LL and RR condensates, each of which break $SU(3)_c \rightarrow SU(2)_c$, are only aligned by a subleading term in the vacuum energy calculation. In a heavy ion collision we might expect the condensates to be misaligned by an arbitrary $SU(3)_c$ transformation, leading to violation of parity and complete breaking of the color group. In the three flavor case we might expect much the same. Here the gauge loop contributions to the vacuum energy from gluon loops will tend to reduce the energy difference between the CFL and, for example, the (1,0,0) condensates as discussed above. The strange quark mass also tends to reduce the energy gap between these two condensates as discussed in [13]. For some (uncalculable) value of m_s of order Λ_{QCD} we expect a phase transition between these two condensates as the number of light flavors changes from 3 to 2. Thus for realistic values of m_s , and densities and temperatures achievable in heavy ion collisions, we might expect disoriented condensates to form with a range of possible color symmetry breaking patterns appearing on a collision by collision basis.

To see how such variation in color symmetry breaking might be seen in an experiment we consider the extreme case where the $SU(2)_c$ subgroup is left unbroken (this is the true vacuum of the two flavor theory). Consider a region which in the wake of a heavy ion collision volume is sufficiently cool and dense to allow the formation of a diquark condensate, with gauge symmetry broken to $SU(2)_c$. The region presumably expands and cool in the usual fashion. However, one color of quark (e.g. red) does not participate in the condensation and its propagator is unaffected by Δ . It is also more weakly interacting since its color corresponds to precisely the broken part of the gauge group (gluons which couple to red quarks are screened by the Meissner effect). The remaining two colors of quarks participate in Cooper pairing and interact strongly with the plasma, so they do not disperse as quickly. The red quarks will therefore tend to flow to the surface of the fireball, providing a mechanism for macroscopic transport of color charge. Note that the condensate is stable under this charge separation since it is the condensate favored by an $SU(2)_c$ theory with two flavors. Furthermore, with $SU(3)_c$ broken to $SU(2)_c$ there is no restoring force which prevents this

charge polarization. On leaving the superconducting volume red quarks will suddenly be required to hadronize because their color charge can now support long range fields and they become aware of the large value of the other two color charges in the center. We expect that this color polarized fireball will hadronize very differently than a quark gluon plasma which is locally color neutral. Naively one expects quark anti-quark production on the boundary of the color charge separation in order to enforce charge neutrality. The separated red charge would then emerge as energetic hadrons, leaving a cooler central region behind.

The scenario described above is the extreme case of a fully unbroken $SU(2)_c$ subgroup. On the other hand a CFL state treats all colors equally and there will be no charge polarization. On an event by event basis we expect variation between these two extremes. The most likely signal of such events is a departure from the standard thermal distribution so far observed in heavy ion collisions [24], both on an event by event basis and averaged over many events.

Acknowledgements: SH would like to thank D.K. Hong, V. Miransky, M. Nowak and M. Rho for useful discussions. Part of this work was performed at the Korean Institute for Advanced Study (KIAS). SH is supported under DOE contract DE-FG06-85ER40224. NJE acknowledges the support of a PPARC Advanced Fellowship. MS is supported under DOE contract DE-FG02-91ER40676. JH is supported in part by the Natural Sciences and Engineering Research Council of Canada and the Fonds pour la Formation de Chercheurs et l'Aide à la Recherche of Québec.

References

- [1] D. Bailin and A. Love, Nucl. Phys. B190 (1981) 175; Nucl. Phys. B190 (1981) 751; Nucl. Phys. B205 (1982) 119; Phys. Rep. 107 (1984) 325).
- [2] M. Alford, K. Rajagopal and F. Wilczek, Phys.Lett. B422, 247 (1998).
- [3] R. Rapp, T. Schäfer, E. V. Shuryak and M. Velkovsky, Phys.Rev.Lett.81, 53 (1998).
- [4] R. Rapp, T. Schäfer, E. V. Shuryak and M. Velkovsky, hep-ph/[A9904353.
- [5] N. Evans, S. D. H. Hsu and M. Schwetz, Nucl.Phys.B551, 275 (1999); Phys.Lett.B449, 281 (1999).
- [6] T. Schäfer and F. Wilczek, Phys.Lett.B450:325-331,1999; hep-ph/9810509.
- [7] D. T. Son, Phys.Rev.D54 094019 (1999).

- [8] R. D. Pisarski and D. H. Rischke, nucl-th/9811104.
- [9] R. D. Pisarski and D. H. Rischke, nucl-th/9903023.
- [10] D. K. Hong, hep-ph/9812510.
- [11] D. K. Hong, hep-ph/9905523.
- [12] D. K. Hong, M. Rho and I. Zahed, hep-ph/9906551.
- [13] M. Alford, K. Rajagopal and F. Wilczek, Nucl.Phys.B537, 443 (1999); M. Alford, J. Berges and K. Rajagopal, hep-ph/9903502.
- [14] J. Berges and K. Rajagopal, Nucl.Phys.B538, 215 (1999).
- [15] S. Hands, J.B. Kogut, M.-P. Lombardo and S.E. Morrison, hep-lat/9902034; S. Hands and S.E. Morrison hep-lat/9902012, hep-lat/990521. J.B. Kogut, M.A. Stephanov and D. Toublan, hep-ph/9906346.
- [16] T. Schäfer and F. Wilczek, PRL 82 (1999) 3956; hep-ph/9903503.
- [17] D.K. Hong, V.A. Miransky, I.A. Shovkovy and L.C.R. Wijewardhana, hep-ph/9906478.
- [18] T. Schäfer and F. Wilczek, hep-ph/9906512.
- [19] R. D. Pisarski and D. H. Rischke, nucl-th/9907041.
- [20] S.D.H. Hsu and M. Schwetz, hep-ph/9908310.
- [21] G. Benfatto and G. Gallavotti, J. Stat. Phys. 59, 541 (1990); Phys. Rev. C42 (1990) 9967; R. Shankar, Physica A177, 530 (1991); Rev. Mod Phys. 66, 129 (1993); J. Polchinski, in Proceedings of the 1992 TASI, eds. J. Harvey and J. Polchinski (World Scientific, Singapore 1993).
- [22] M. Le Bellac, Thermal Field Theory, Cambridge University Press, Cambridge, 1996.
- [23] J.M. Cornwall, R. Jackiw and E. Tomboulis, PRD10, 2428 (1974).
- [24] F. Becattini, M. Gazdzicki, J. Sollfrank, Nucl. Phys. Proc. Suppl. 71 324 (1999); F. Becattini, M. Gazdzicki, J. Sollfrank, Nucl. Phys. A638 403 (1998).